

## Research Article

**Herbal Compound Farnesiferol C Exerts Antiangiogenic and Antitumor Activity and Targets Multiple Aspects of VEGFR1 (Flt1) or VEGFR2 (Flk1) Signaling Cascades**

Jae-Ho Lee<sup>1</sup>, Sun Choi<sup>2</sup>, Yoonji Lee<sup>2</sup>, Hyo-Jeong Lee<sup>1,3</sup>, Kwan-Hyun Kim<sup>1</sup>, Kyoo-Seok Ahn<sup>1</sup>, Hyunsoo Bae<sup>1</sup>, Hyo-Jung Lee<sup>1</sup>, Eun-Ok Lee<sup>1</sup>, Kwang-Seok Ahn<sup>1</sup>, Shi Yong Ryu<sup>4</sup>, Junxuan Lü<sup>3</sup>, and Sung-Hoon Kim<sup>1,3</sup>

**Abstract**

Farnesiferol C (FC) is one of the major compounds isolated from *Ferula assafoetida*, an Asian herbal spice used for cancer treatment as a folk remedy. Here, we examined the hypothesis that novel antiangiogenic activities of FC contribute to anticancer efficacy. In human umbilical vein endothelial cells (HUVEC), exposure to the 10 to 40  $\mu\text{mol/L}$  concentration range of FC inhibited vascular endothelial growth factor (VEGF)-induced cell proliferation, migration, invasion, tube formation, and the expression of matrix metalloproteinase-2. In addition, FC inhibited the angiogenic sprouting of VEGF-treated rat aorta in an *ex vivo* model. Furthermore, FC inhibited the *in vivo* growth of mouse Lewis lung cancer allograft model by 60% ( $P < 0.001$ ) at a daily i.p. dosage of 1 mg/kg body weight without any negative effect on the weight of the host mice. Immunohistochemistry staining showed decreased microvessel density (CD34) and proliferative index (Ki-67) without affecting the apoptotic (terminal deoxynucleotidyl transferase-mediated dUTP nick end labeling) index. Mechanistically, FC decreased the binding of VEGF to VEGFR1/Flt-1, but not to VEGFR2/KDR/Flk-1. In terms of early signaling, FC exerted a rapid inhibitory action (examined within 10 minutes) on VEGF-induced autophosphorylation of VEGFR1 without affecting that of VEGFR2. Nevertheless, FC decreased the phosphorylation of most of the kinases downstream of VEGFR2: focal adhesion kinase, Src, extracellular signal-regulated kinase 1/2, p38 mitogen-activated protein kinase, and *c-jun*-NH<sub>2</sub>-kinase without affecting AKT. Computer simulation suggests that FC may inhibit Src or focal adhesion kinase protein activities directly through its docking to their ATP-binding sites. Taken together, the multitargeting actions of FC, particularly VEGFR1 inhibition, may make it a novel drug candidate to complement current VEGF/VEGFR2-targeting antiangiogenic modalities for cancer. *Mol Cancer Ther*; 9(2); 389–99. ©2010 AACR.

**Introduction**

Farnesiferol C (FC) is one of the sesquiterpene coumarin compounds isolated from the resin of *Ferula assafoetida* L., which is used as a food spice in many Asian countries and for the treatment of asthma, bronchitis, ulcer, kidney

**Authors' Affiliations:** <sup>1</sup>Cancer Preventive Material Development Research Center, College of Oriental Medicine, Kyunghee University and <sup>2</sup>College of Pharmacy, National Core Research Center for Cell Signaling and Drug Discovery, Ewha Womans University, Seoul, Korea; <sup>3</sup>The Hormel Institute, University of Minnesota, Austin, Minnesota; and <sup>4</sup>Korea Research Institute of Chemical Technology, Yuseong-gu, Daejeon, Korea

**Note:** Supplementary material for this article is available at Molecular Cancer Therapeutics Online (<http://mct.aacrjournals.org/>).

J. Lü holds a Kyung Hee University International Scholar travel award, 2009 to 2010.

J.-H. Lee and S. Choi contributed equally to this work and should be considered co-first authors.

**Corresponding Authors:** Sung-Hoon Kim, College of Oriental Medicine, Kyunghee University, 1 Hoegi-dong, Dongdaemun-gu, Seoul 131-701, Republic of Korea. E-mail: [sungkim7@khu.ac.kr](mailto:sungkim7@khu.ac.kr) or Junxuan Lü, Hormel Institute, University of Minnesota, 801 16th Avenue Northeast, Austin, MN 55912. Phone: 507-437-9680; Fax: 507-437-9606. E-mail: [ju@hi.umn.edu](mailto:ju@hi.umn.edu)

doi: 10.1158/1535-7163.MCT-09-0775

©2010 American Association for Cancer Research.

stone, pain, and cancer in traditional herbal medicine. *F. assafoetida* L. was reported to have antitumor (1, 2), antimutagenic (2), and antiviral activities (3). The underlying mechanism of its antitumor activity and the active chemical(s) remain unclear. Considering that some coumarin compounds have been reported to possess antiangiogenic activity (4–7) and that angiogenesis is critical for cancer growth and progression (8, 9), we sought to test the hypothesis that FC might exert antiangiogenic activity to contribute to the cancer therapeutic or preventive effect.

Angiogenesis involves the growth of new blood vessels from preexisting vessels (8, 9). The angiogenic responses involve many biochemical and molecular signaling events and complex cellular processes, such as endothelial cell proliferation, directional migration, basement membrane degradation, and remodeling by matrix metalloproteinase (especially MMP-2), capillary tube formation, and differentiation (10, 11). Vascular endothelial growth factor (VEGF) is a potent proangiogenic factor crucial for tumor vascular development (12–14). Of the VEGF families of proteins, VEGF-A isoforms such as VEGF<sub>165</sub> and VEGF<sub>121</sub> exert mitogenic and proangiogenic actions on the endothelial cells through binding to membrane

protein tyrosine kinase receptors expressed on endothelial cells, including VEGFR1 (also known as Flt-1 for Fms-like tyrosine kinase-1) and VEGFR2 (also known as Flk-1 for fetal liver kinase-1 or KDR for kinase insert domain-containing receptor; refs. 12, 14, 15). VEGFR2 is by far the most important receptor for VEGF-A signaling in vascular endothelial cells (12).

Clinical trials in the last few years with antiangiogenic modalities targeting VEGF-A/VEGFR2 using inactivating monoclonal antibodies or kinase inhibitor drugs as single agents or in combination with chemotherapy have shown some survival benefit in cancer patients of an increasing number of advanced-stage malignancies (16). However, the benefits are at best transitory and are followed by restoration of tumor growth and progression. Major hurdles for clinical implementation include limited efficacy, rapid development of escape, and resistance to the antiangiogenic modalities; in rare cases, severe toxicity may occur, arising from VEGF-A/VEGFR2 ablation-induced severe hypoxia and its complications (16, 17). On the other hand, VEGFR1 is expressed not only in endothelial cells but also in many other cell types, such as macrophages, stromal cells, pericytes, smooth muscle cells, tumor cells, dendritic cells, bone marrow progenitors, and leukemic cells (17). VEGFR1 binds placental growth factor and VEGF-B in addition to VEGF-A. Naturally occurring soluble nonsignaling VEGFR1 or genetically engineered VEGFR1 serve as traps for VEGF-A due to the much tighter binding than VEGFR2 for VEGF-A (17). As more mechanistic studies reveal that the ligand specificity and signaling consequences for the VEGFRs are not equivalent and important cross-talks among different ligand-VEGFR signaling cascades within and among endothelial and many other cell types comprise the tumor angiogenesis environment, approaches targeting other VEGFRs and ligand signaling may complement the existing VEGF/VEGFR2 antiangiogenesis modalities to improve the cancer treatment efficacy and patient safety (16, 17). Toward this end, small molecular compounds that target different VEGFRs will add to the arsenal of antiangiogenesis drug leads. We and others have shown that small-molecule angiogenesis inhibitors present in Oriental herbs that interfere with VEGF-A/VEGFR signaling could be potentially valuable for antiangiogenic treatment of cancer in preclinical models (18–22).

In the present study, we investigated the antiangiogenic attributes of FC in VEGF-A-stimulated human umbilical vein endothelial cell (HUVEC) model and its efficacy against the sprouting of VEGF-treated rat aortic endothelial cells in an *ex vivo* model. We established its *in vivo* anticancer effect in the highly angiogenic Lewis lung cancer (LLC) allograft model. In addition, we examined associated molecular mechanisms in terms of VEGF/VEGFR1/2 binding and VEGFR kinase signaling cascades. We report here data suggesting a differential targeting by FC of the VEGFR1 and VEGFR2 signaling axis. Furthermore, computational docking simulations with Src kinase and focal adhesion kinase (FAK) proteins suggest possible direct inhibition of their kinase activities by FC.

## Materials and Methods

### Isolation of FC from *F. assafoetida* L.

Dried *F. assafoetida* L. (1.2 kg) was extracted with methanol. The methanol extract (460 g) was successively fractionated with *n*-hexane, dichloromethane, and *n*-butanol. Each fraction was evaporated under vacuum. Further separation of the dichloromethane fraction (5 g) was done using silica gel column chromatography (Merck Kieselgel 60, 70–230 mesh, 300 g) with dichloromethane/methanol solution (100:1–10:1) as an eluent to yield four fractions (Fr.1–Fr.4). Among them, Fr.3 was chromatographed on a silica gel column using *n*-hexane/ethyl acetate (4:1–1:1) as an eluent to yield subfractions. Subfractions were further separated through a Sephadex LH-20 (ethyl acetate/methanol, 10:1) and purified by high performance liquid chromatography JAI-ODS column using methanol to yield crystalline (purity >99%) FC [400 mg; colorless needle, mp 82°C,  $[\alpha]_D^{25}$ -36 (c, 1.0 in CHCl<sub>3</sub>), C<sub>24</sub>H<sub>30</sub>O<sub>4</sub>, MW 382]. The chemical structure is shown in Fig. 1A. Results of spectral analyses are shown in Supplementary Fig. S1.

FC was dissolved in dimethyl sulfoxide for the *in vitro* studies and dissolved in dimethyl sulfoxide then diluted with PBS for the *in vivo* study.

### Cell Culture

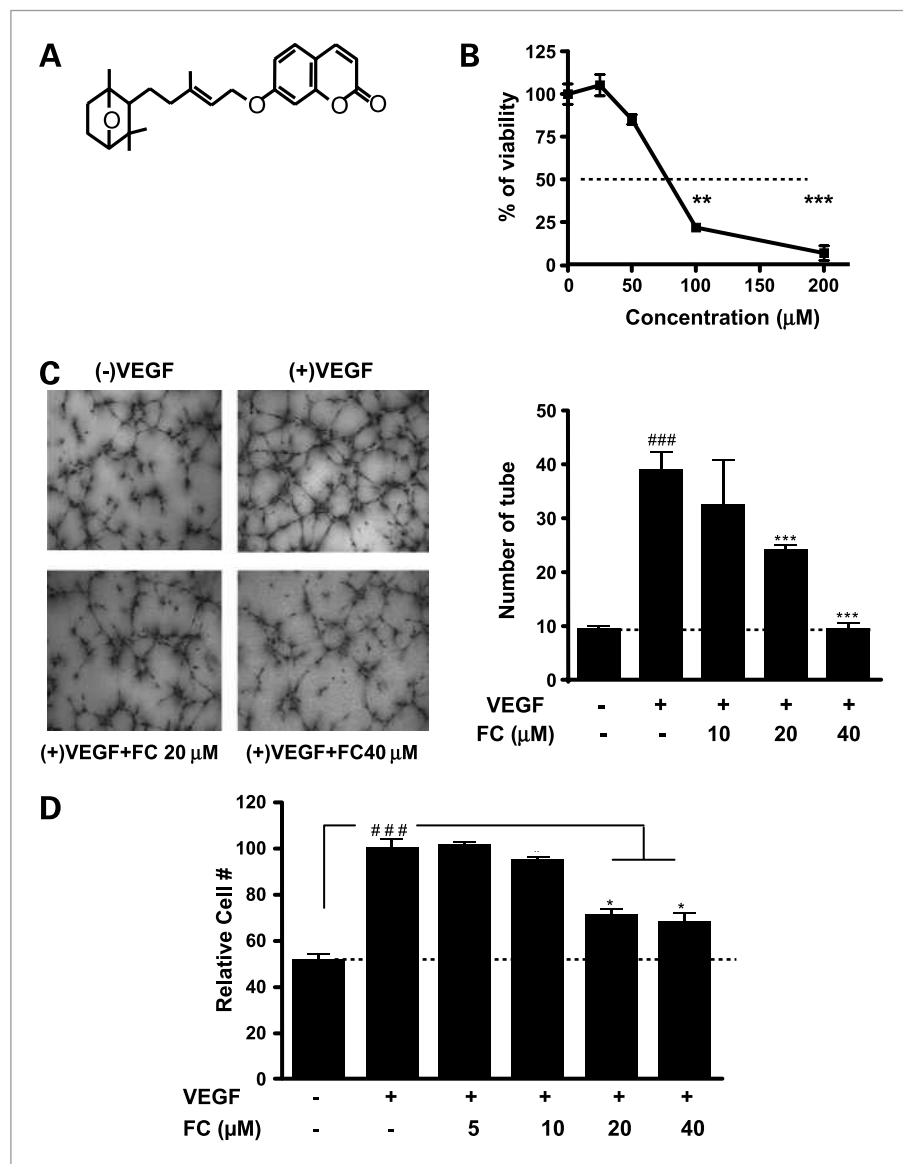
HUVECs were prepared from primary culture of human umbilical cord veins as we have described previously (18). The adherent (culture flasks were coated with 0.1% gelatin) endothelial cells were maintained in M199 medium plus 20% heat-inactivated fetal bovine serum (FBS, Gibco), 3 μg/mL of basic fibroblast growth factor, 100 units/mL of penicillin/streptomycin, and 2 mmol/L L-glutamine (complete medium) and incubated at 37°C in 5% CO<sub>2</sub>. Once confluent, the cells were detached by trypsin-EDTA solution and used in experiments from the third to the sixth passages. Mouse Lewis lung carcinoma (LLC) cells were kindly provided by Dr. K. Takeda (Tohoku University, Tohoku, Japan). They were maintained as monolayer cultures in Eagle's minimal essential medium (Gibco) supplemented with 10% FBS. LLC cells were collected by brief treatment with trypsin-EDTA and used for the *in vivo* experiment.

The following assays were routinely used by our laboratories. Cytotoxicity and cell proliferation assays for HUVECs were carried out with the metabolic dye 2,3-bis[2-(4-nitro-5-sulfophenyl)-2H-tetrazolium-5-carboxanilide (XTT) as we have reported previously (18). HUVEC tube formation assay, Western blotting, and immunohistochemistry were carried out essentially as reported previously (18, 20).

### Motility Assay

Motility assay for HUVECs was based on "scratch" wounding a confluent monolayer (23). HUVECs (3 × 10<sup>5</sup>) were seeded onto 0.1% gelatin-coated six-well plates in complete medium until a confluent monolayer was formed. The cells were scratch wounded using the tip

**Figure 1.** A, structure of FC. B, cytotoxic effect of FC on HUVECs under nonproliferative conditions. HUVEC cells were exposed to FC in M199 medium containing 5% FBS (without heparin and growth factors) for 24 h and the proportion of metabolically viable cells was assessed by the XTT assay. Mean  $\pm$  SEM,  $n = 3$ . \*\*\*,  $P < 0.01$ ; \*\*\*\*,  $P < 0.001$  compared with control. C, effect of FC on VEGF-induced tube formation (18-h stimulation in the absence or presence of FC). Data in graph were presented as mean  $\pm$  SEM,  $n = 5$  fields. ###,  $P < 0.001$  compared with basal control; \*\*\*,  $P < 0.001$  compared with VEGF-stimulated group. D, effect of FC on VEGF-A (10 ng/mL)-induced proliferation of HUVECs for 48 h. The relative number of metabolically viable cells were estimated by the XTT assay. Data were means  $\pm$  SEM,  $n = 3$  independent wells. ###,  $P < 0.001$  compared with basal control; \*,  $P < 0.05$  compared with VEGF-stimulated group.



of a universal 200  $\mu\text{L}$  pipette tip. Then, cells were treated with FC in M199 with 5% FBS, 10 ng/mL VEGF, and 5 units/mL heparin. After 16-h incubation, the cells were rinsed with PBS and stained in Diff Quick solution, and randomly chosen fields were photographed under a light microscope at  $\times 200$  magnification. The number of migrated cells was counted.

### Invasion Assay

Invasion assay was done using modified Boyden chamber as we have described previously (20) using Matrigel (BD Bioscience)-coated polycarbonate Nucleopore membrane (Corning; 8- $\mu\text{m}$  pore size). Serum-free M199 medium containing VEGF (10 ng/mL) was pipetted into the lower wells. HUVECs were trypsinized and suspended at a density of  $1 \times 10^5$  cells/100  $\mu\text{L}$  in the

serum-free M199 medium without VEGF. Then, the cells were pretreated with FC for 30 min at room temperature and 100  $\mu\text{L}$  of the cell suspension were loaded into the upper wells. The chamber was incubated in 5%  $\text{CO}_2$  at 37°C. After 12-h incubation, the membrane was fixed and stained with Diff-Quick solution. Invasiveness was determined by counting the cells that have passed through the filter.

### Gelatin Zymography

We detected secreted pro-MMP-2 in HUVEC conditioned medium essentially as described by Jiang and colleagues (24). HUVECs (80% confluent) were washed with serum-free M199 and incubated with or without VEGF (10 ng/mL) containing FC for 20 h. The proteins in conditioned medium were size fractionated on a 10%

SDS-polyacrylamide gel impregnated with 0.1% gelatin. Next, MMP2 and other MMPs were activated in gel for 18 h at 37°C. Gels were fixed, stained with 0.25% Coomassie brilliant blue R250, and destained. Gelatinase activity was visualized as cleared band on the stained gel.

### VEGFR Binding Assay

We performed the assay following a protocol by Lee et al. (19). VEGF (50 ng/well) in 50  $\mu$ L of PBS were immobilized to 96-well plates. The wells were washed and blocked with 3% bovine serum albumin in PBS for 2 h. FC with 1% bovine serum albumin in PBS were added with Flt-1-Fc (VEGFR1) or KDR/Flk-1 (VEGFR2; 25 ng/mL) to VEGF-coated wells. After 2-h incubation, the wells were washed thrice with PBST. Flt-1 or KDR/Flk-1 bound to VEGF was determined by biotinylated anti-human IgG (Dako) and horseradish peroxidase-conjugated streptavidin (Sigma), developed with tetramethylbenzidine substrate reagent (BD Biosciences), and quantified by measuring the absorbance at 450 nm.

### Aortic Ring Assay

We used tissues from 6-wk-old male Sprague-Dawley rats essentially as described by Kruger et al. (25). The aortic rings were placed into the wells of plates (48-well) coated with 150  $\mu$ L of Matrigel and sealed in place with an overlay of 50  $\mu$ L of Matrigel. VEGF with or without FC was added to the wells in a final volume of 200  $\mu$ L of serum-free M199 medium, whereas medium alone was used as basal control. On day 6, the aortic ring cells were fixed and stained with Diff-Quick. The number of sprouts was counted.

### In vitro Kinase Activity

We measured endogenous Src kinase according to the manufacturer's instructions (Upstate Biotechnology). In brief, the supernatant containing 200  $\mu$ g of protein per sample, derived from HUVECs that were stimulated with VEGF (10 min) in the absence or presence of FC (pretreated 30 min), was incubated with 1  $\mu$ g of Src monoclonal antibody at 4°C overnight. Immunoprecipitated Src was incubated in optimized buffer (with 0.2  $\mu$ Ci of [ $\gamma$ -<sup>32</sup>P]ATP) for 30 min at 30°C with agitation. The reaction was stopped by adding trichloroacetic acid, and an aliquot was transferred onto P81 paper square. The assay squares were washed and were transferred to a scintillation vial for scintillation counting. The activity of the recombinant enzyme was determined by using 20 ng of purified active form of Src kinase (Upstate Biotechnology).

### LLC Allograft Tumor Model

We carried out *in vivo* studies as described previously (18, 20). Five-week-old female C57BL/6 mice were purchased from Daehan Biolink and given food and water *ad libitum*. Mice were housed in a room maintained at 25  $\pm$  1°C with 55% relative humidity. Each group consisted of 10 mice. One week later, LLC cells ( $3 \times 10^5$ ) in

200  $\mu$ L PBS were s.c. inoculated into the right flank of mice. Five days after LLC inoculation, mice were given an i.p. injection of FC at doses of 0.1 and 1 mg/kg daily for 12 d, whereas control mice were administered with PBS. These dosages were chosen based on an assumption of achieving circulating levels of FC modeled in the *in vitro* models to exert antiangiogenic action as the primary mediating mechanism against tumor growth.

### Molecular Modeling

The coordinates of the protein structures were obtained from the Protein Data Bank: 1Y57 (26) for active Src tyrosine kinase, 2H8H (27) for inactive Src kinase, and 2IJM for FAK.<sup>5</sup> The protein structures were aligned with Align Structures by Homology Module in SYBYL molecular modeling program (Tripos International). 1Y57 was used as a fixed reference protein, and the rest of the protein structures were aligned onto 1Y57 based on their  $\alpha$  carbons.

The X-ray crystal structures were prepared using the Biopolymer Structure Preparation Tool in SYBYL and used for flexible docking studies with Surflex-Dock (28) implemented in SYBYL. The crystal ligand was used to define the active site for Surflex-Dock (using ligand mode), which uses an idealized active site called a protocol, built from the hydrogen-containing protein mol2 file and based on protein residues that line the active site using standard variables. The three-dimensional structures of tested molecules were generated with Concord and energy minimized using the MMFF94s force field (method, Powell; termination gradient, 0.05 kcal/mol  $\text{\AA}$ ; max iterations,  $1 \times 10^6$ ) in SYBYL. Surflex-Dock was run using default settings (except additional starting conformations per molecule of 10), and the 50 best-docked poses for each ligand were analyzed. All computational studies were done with the Tripos SYBYL molecular modeling program package, version 8.0.2, on a Linux (RHEL 4.0 Intel Xeon processor 5050) workstation.

### Statistical Analysis

All data were presented as means  $\pm$  SD or SEM. The statistical significance of differences among groups was evaluated by ANOVA.

### Results

#### Defining the Cytotoxic Range of FC against Nonproliferative HUVECs

The cytotoxic activity of FC against HUVECs was assessed without the supplementation of angiogenic factors in 5% FBS-containing M199 medium (condition did not support proliferation). FC treatment for 24 hours caused

<sup>5</sup> C.C. Lee. Crystal structure of focal adhesion kinase domain with 2 molecules in the asymmetric unit complexed with ADP and ATP. 2007. <http://www.cbi.ac.uk/pdbsum/2ijm>.



a modest decrease in the percentage of metabolically viable HUVECs at 50  $\mu\text{mol/L}$ , and greatly decreased viability at 100 and 200  $\mu\text{mol/L}$  (Fig. 1B). The concentration for 50% inhibition ( $\text{IC}_{50}$ ) of viability was  $\sim 70$   $\mu\text{mol/L}$ .

### Effect of FC on VEGF-Induced HUVEC Tube Formation

A well-known *in vitro* angiogenesis test is "tube formation" by HUVECs into interconnected cords when seeded

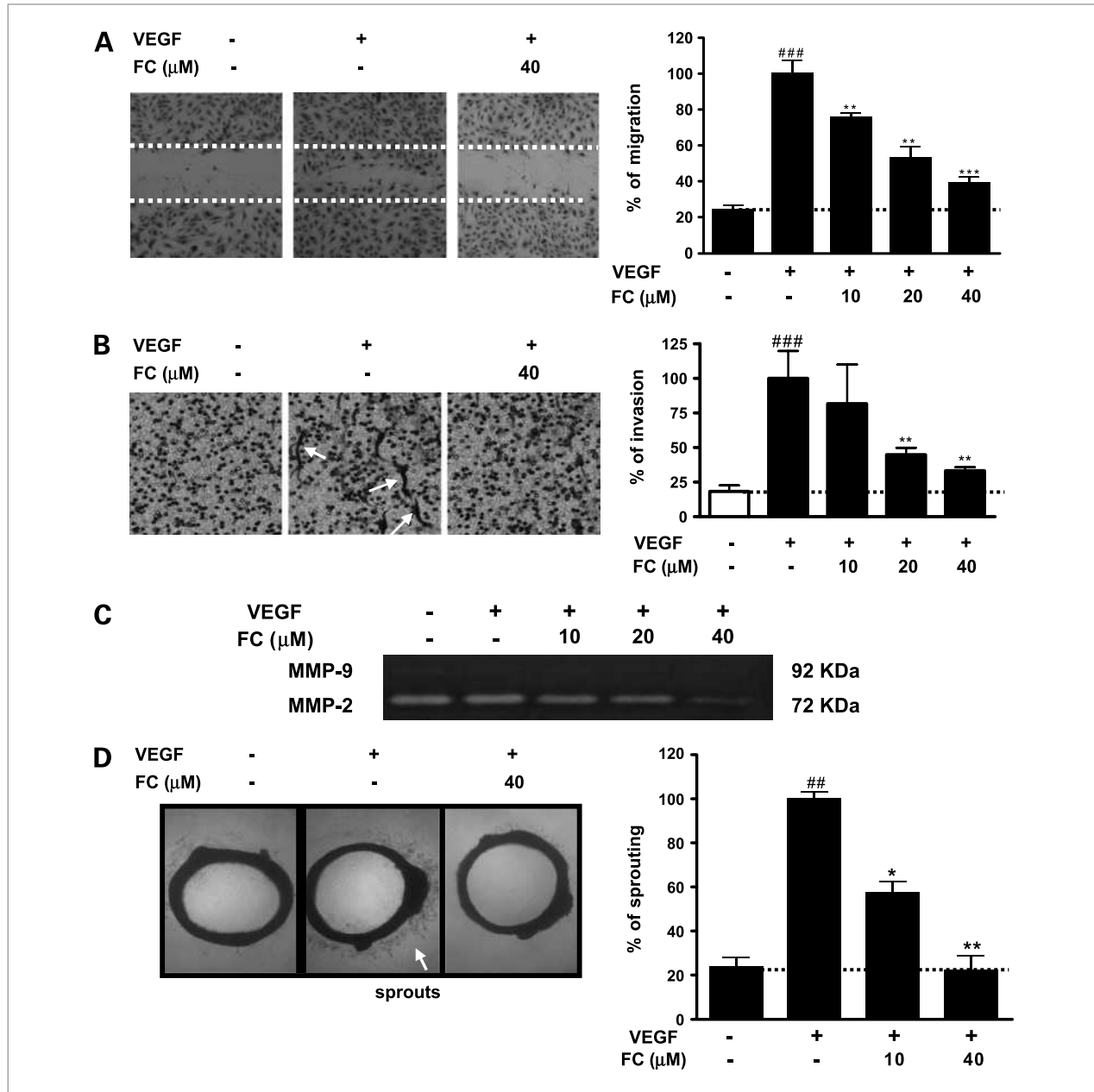


**Figure 2.** A, effect of FC on VEGF-induced cell motility (wound-healing test). Confluent HUVEC monolayers on 0.1% gelatin-coated six-well plates were scratch wounded. The cells were treated with various concentrations of FC in M199 with 5% FBS, 10 ng/mL VEGF, and 5 units/mL heparin for 16 h. Representative fields were photographed,  $\times 100$  magnification. Graph shows the quantitative effect of FC on VEGF-induced HUVEC motility. Data were presented as mean  $\pm$  SEM,  $n = 3$  wells. <sup>###</sup>,  $P < 0.001$  compared with basal control; <sup>\*\*</sup>,  $P < 0.01$ ; <sup>\*\*\*</sup>,  $P < 0.001$  versus VEGF-stimulated group. B, effect of FC on VEGF-induced invasion of HUVEC through Matrigel in 12 h. Data were presented as means  $\pm$  SEM  $n = 3$  wells. <sup>###</sup>,  $P < 0.001$  compared with basal control; <sup>\*\*</sup>,  $P < 0.01$  compared with VEGF-stimulated group. C, effect of FC on VEGF-induced MMP-2 secretion from HUVECs after 20 h examined by zymography. D, effect of FC on VEGF-induced vessel sprouting *ex vivo* from rat aortic segments. Rat aortic segments were cultured on Matrigel and treated with VEGF (20 ng/mL) in the absence or presence of FC for 6 d. Graph shows the endothelial sprouts counts as the relative ratio to VEGF-stimulated control as 100. Data were presented as mean  $\pm$  SEM,  $n = 3$  aortas. <sup>##</sup>,  $P < 0.01$  compared with basal control; <sup>\*</sup>,  $P < 0.05$  and <sup>\*\*</sup>,  $P < 0.01$  compared with VEGF-stimulated control.

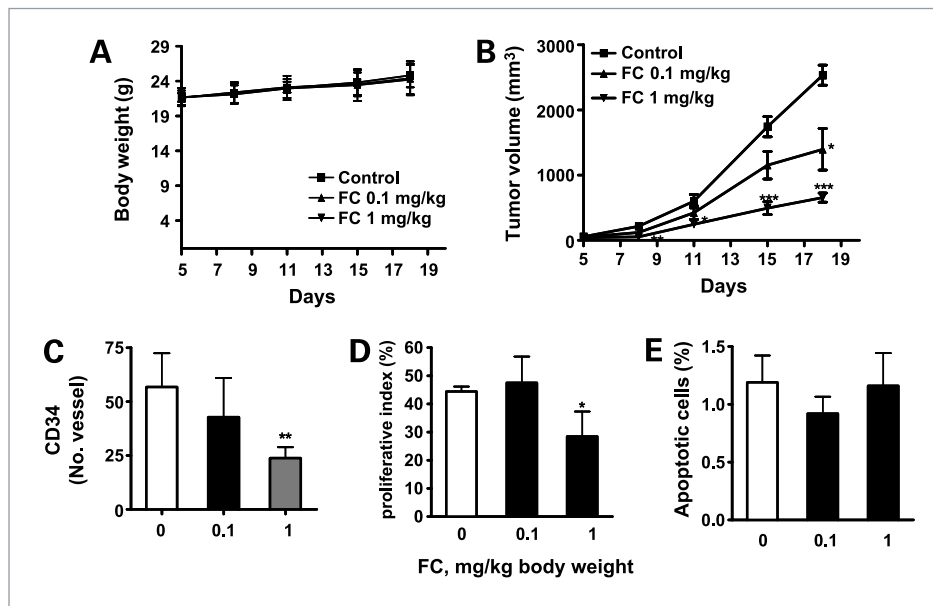


**Figure 3.** Effect of FC on the *in vivo* growth of LLC allograft tumors in mice and on angiogenesis and proliferation indices. LLC cells ( $5 \times 10^5$ ) were injected s.c. into the right flank of C57BL/6 mice. After 5 d, mice were given i.p. injection of FC (0.1 mg/kg and 1 mg/kg) or PBS (control) once a day. A, body weights of mice. B, tumor growth over time. Mean  $\pm$  SD,  $n = 10$  mice per group. \*,  $P < 0.05$ ; \*\*,  $P < 0.01$ ; \*\*\*,  $P < 0.001$  compared with control. C, CD34 index (angiogenesis). D, Ki67 index (proliferation), E, TUNEL index (apoptosis). \*,  $P < 0.05$ ; \*\*,  $P < 0.01$  compared with control. Mean  $\pm$  SD,  $n = 10$ .

on Matrigel. We examined whether FC inhibited VEGF-A–promoted tube formation of HUVECs, focusing on the concentration range of 10 to 40  $\mu\text{mol/L}$ . Endothelial cells stimulated by VEGF-A (10 ng/mL) on Matrigel became much better organized than the unstimulated cells (Fig. 1C), as evidenced by the length and thickness of the cords and the complexity of the branching structures. FC treatment inhibited the VEGF-A–promoted tube formation of HUVECs in a concentration-dependent manner (Fig. 1C), with  $\text{IC}_{50}$  of 20  $\mu\text{mol/L}$  and a complete reversal to baseline at 40  $\mu\text{mol/L}$ . These data suggested that FC might interfere with critical cellular processes mediating the *in vitro* angiogenic responses to VEGF without overt cytotoxicity.

#### Effect of FC on VEGF-Induced Proliferation of HUVECs

Vascular endothelial cells in existing blood vessels usually remain quiescent until stimulated by angiogenic factors to proliferate. As shown in Fig. 1D, VEGF-A (10 ng/mL) stimulation for 48 h increased the number of HUVECs ~2-fold. FC inhibited VEGF-induced increment of XTT-viable HUVECs above the unstimulated baseline by >60% at 20  $\mu\text{mol/L}$  when compared with VEGF stimulation alone. The  $\text{IC}_{50}$  of FC to inhibit the VEGF-induced increment of cell proliferation was ~15  $\mu\text{mol/L}$ .

#### Effect of FC on VEGF-Induced Migration, Invasion, and MMP-2 Secretion of HUVECs

Motility and migration of vascular endothelial cells are important in the angiogenic sprouting process. To determine the effects of FC on endothelial cell migration stimulated by VEGF, we scraped confluent monolayers of HUVECs to clear space for motile cells to move into. As shown in Fig. 2A, in the absence of VEGF, HUVEC

cells did not fill the gap even after 16 hours of “wounding” the monolayer. Stimulation by VEGF-A (10 ng/mL) for 16 hours increased HUVEC motility to nearly fill in the gap. FC inhibited VEGF-induced migration of HUVECs, with half-maximal inhibition at ~20  $\mu\text{mol/L}$  (Fig. 2A, graph).

Because directional motility and matrix degradation are crucial for angiogenesis sprouting, we next examined whether FC affected the invasion ability of HUVECs using the Boyden chamber assay, which required cells to degrade and migrate through a sheet of extracellular matrix on a Matrigel-coated membrane. As shown in Fig. 2B, VEGF induced a 5-fold increase of HUVECs that passed the filter in 12 hours, and this effect was decreased by FC, with  $\text{IC}_{50}$  below 20  $\mu\text{mol/L}$  (graph).

Because invasion requires the degradation of extracellular matrix components, we examined the effect of FC on the secretion of pro-MMP-2 from HUVECs using a zymography assay (Fig. 2C). The protease secretion was inhibited by FC with  $\text{IC}_{50}$  of ~20  $\mu\text{mol/L}$ .

#### Effect of FC on VEGF-Induced Vessel Sprouting *Ex vivo*

The above experiments have revealed significant inhibitory actions of FC on a number of VEGF-induced molecular signaling pathways and cellular processes in HUVECs in the absence of other cell types or organ structural context. We next did an *ex vivo* aortic ring angiogenesis sprouting assay to confirm the antiangiogenic activity of FC when the target endothelial cells were organized in the three-dimensional organ context of the aorta. VEGF (20 ng/mL) significantly stimulated vessel sprouting (Fig. 2D, middle image, meshwork of lightly stained capillaries marked by arrow). The VEGF-stimulated sprouting was inhibited by FC with an  $\text{IC}_{50}$  of ~10  $\mu\text{mol/L}$  (Fig. 2D, graph).

### Effect of FC on Tumor Growth *In vivo*

Prompted by the *in vitro* and *ex vivo* data supporting a potential antiangiogenic activity of FC, we examined the *in vivo* efficacy of FC on the growth of mouse Lewis lung cancer (LLC) allograft, which is highly dependent on angiogenesis. The FC-treated groups (0.1 and 1 mg/kg) showed slower growth kinetics of LLC allografts than those in the control group (Fig. 3B). The final tumor weight was decreased in a dose-dependent manner by FC (2.73 g  $\pm$  0.13, 1.87 g  $\pm$  0.42, and 1.10 g  $\pm$  0.17, respectively), being highly statistically significant at the 1 mg/kg dose ( $P < 0.001$ ). FC did not cause reduced body weight of the host mice (Fig. 3A) or other side effects such as hair loss, mortality, and lethargy.

### Effect of FC on *In vivo* Indices of Angiogenesis, Proliferation, and Apoptosis

We examined CD34 staining for newly formed blood vessels, terminal deoxynucleotidyl transferase-mediated dUTP nick end labeling (TUNEL) index for apoptosis, and Ki67 staining index for cellular proliferation (see Supplementary Fig. S2 for staining patterns). Treatment by FC caused a dose-dependent trend of reduction of microvessel density by FC, with 1 mg/kg dose producing a statistically significant reduction (Fig. 3C). Furthermore, FC treatment at the effective dose of 1 mg/kg significantly decreased the Ki-67 index *in vivo* (Fig. 3D). However, TUNEL staining for apoptosis showed no difference between FC-treated groups and control group (Fig. 3E).

To understand the molecular signaling mechanisms involved in accounting for the antiangiogenic and antitumor actions of FC established above, we focused subsequent efforts on the VEGF-VEGFR signaling pathways.

### Differential Effect of FC on the Binding of VEGF to Its Receptors

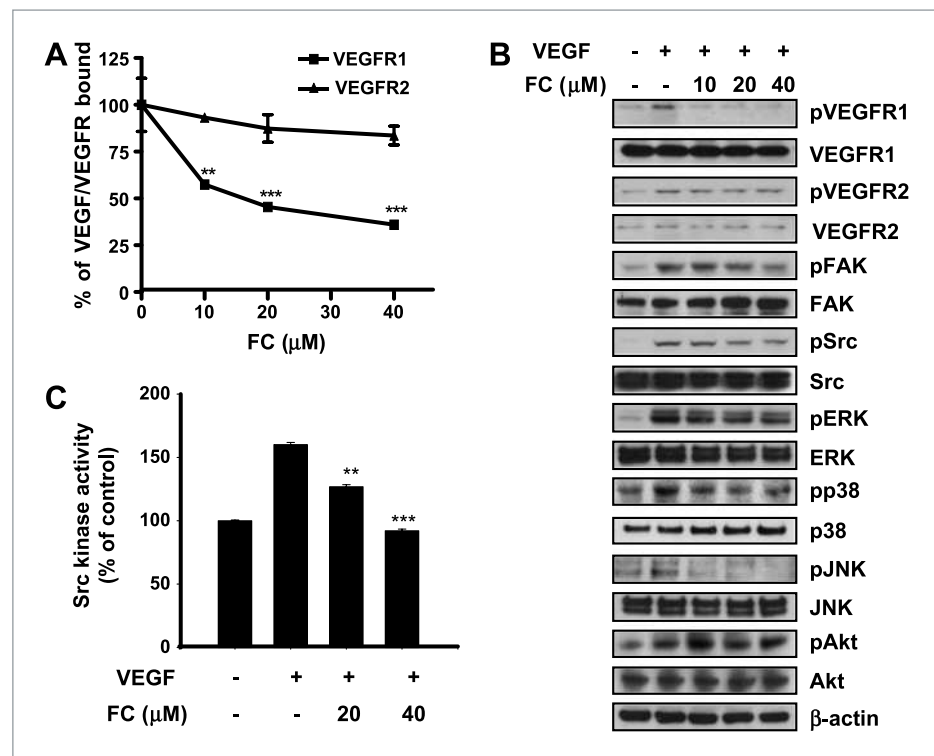
Next, we investigated whether FC inhibited the binding of VEGF to its receptors, VEGFR1 (Flt-1, high affinity) and VEGFR2 (Flk-1/KDR, low affinity). As shown in Fig. 4A, FC decreased the binding of VEGFR1 to immobilized VEGF with  $IC_{50}$  of  $\sim 15 \mu\text{mol/L}$ . However, FC did not affect the binding between VEGF and VEGFR2 (Fig. 4A).

### Effect of FC on VEGFR Downstream Signaling

We examined the effect of FC on VEGFR autophosphorylation (activation) stimulated by VEGF and the immediate downstream signaling cascades. We treated HUVECs with FC for 30 min and then stimulated with 10 ng/mL VEGF for 10 additional minutes. As shown in Fig. 4B, FC nullified VEGF-induced VEGFR1 autophosphorylation at a concentration of as low as 10  $\mu\text{mol/L}$ .

However, FC did not inhibit VEGF-induced VEGFR2 autophosphorylation nor did it affect VEGFR2 protein abundance. FC inhibited VEGF-induced phosphorylation of p125 FAK (pY861) and Src (pY416) in a concentration-dependent manner with an  $IC_{50}$  of  $\sim 20 \mu\text{mol/L}$  (Fig. 4B). FC also inhibited VEGF-induced phosphorylation of extracellular signal-regulated kinase 1/2 (ERK1/2), p38

**Figure 4.** A, effect of FC on the binding of VEGFR1 (Flt-1) and VEGFR2 (KDR/Flk-1) to immobilized VEGF. Data were presented as means  $\pm$  SEM,  $n = 3$ . \*\*,  $P < 0.01$ ; \*\*\*,  $P < 0.001$  compared with control. B, Western blot analyses of effect of FC on VEGFR-signaling kinases. HUVECs were pretreated with FC for 30 min and further stimulated with 10 ng VEGF/mL for 10 min. C, *in vitro* Src kinase activity of FC-treated HUVEC cells prepared as in B.



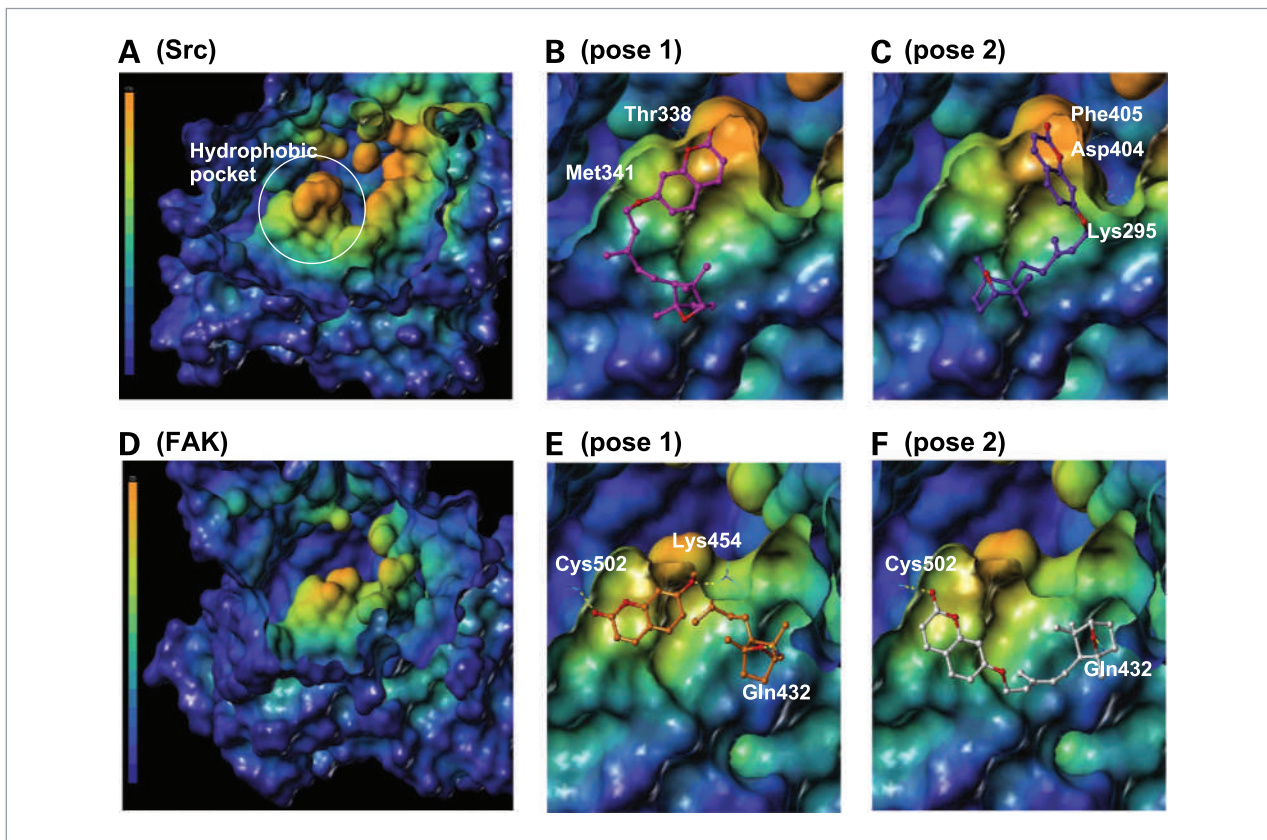


**Figure 5.** The potential binding modes (poses) of FC at the active site of Src tyrosine kinase (A–C) and FAK (D–F) by docking simulation. A and D, hydrophobic pocket near the ATP-binding site in Src and FAK, respectively. Connolly surface was generated for the protein by MOLCAD and colored by cavity depth, in which orange means deep cavity of the hydrophobic pocket. B and C, two possible binding modes of FC in Src. E and F, two possible binding modes of FC in FAK. FC is displayed in ball-and-stick and its carbon colors are magenta/purple in Src and orange/white in FAK, respectively. The Connolly surface was Z-clipped and the nonpolar hydrogen atoms are not displayed for clarity. Hydrogen bonds are displayed as yellow dashed lines and the participating residues are marked.

mitogen-activated protein kinase (MAPK), and *c-jun*-NH<sub>2</sub>-kinase (JNK) in a concentration-dependent manner, in particular most potently against JNK (Fig. 4B). In contrast, FC did not inhibit VEGF-induced AKT phosphorylation although phosphoinositide 3-kinase (PI3K)–AKT activation was a well-established response of HUVECs to VEGF-A/VEGFR2 stimulation. Because most of these changes belong to the VEGFR2-regulated downstream kinase pathways, these data therefore suggest that FC selectively targeted some (e.g., Src, FAK), but not all (e.g., PI3K–AKT), signaling events downstream of VEGFR2, but not VEGFR2 autophosphorylation (activation) itself.

#### Effect of FC on Src Kinase Activity

To confirm that the decreased phosphorylation of key VEGFR2 downstream kinases translated into decreased enzyme activities, we subjected lysates of FC-treated HUVECs to immunoprecipitation with anti-Src antibody and tested the *in vitro* kinase activity using Src substrate peptide. As shown in Fig. 4C, VEGF significantly in-

creased Src kinase activity as expected, and the enzyme activity was decreased by pretreatment of HUVECs with FC in a concentration-dependent manner (Fig. 4C), in parallel with the Src phosphorylation decline (Fig. 4B).

To determine whether FAK and Src phosphorylation was also decreased by FC treatment *in vivo*, we analyzed LLC tumor sections by immunohistochemical staining. Data (Supplementary Fig. S3) are consistent with likely targeting of these two key kinases *in vivo* by FC.

#### Docking Simulations with Src and FAK

To provide insights into how FC might affect Src and FAK enzyme activity without affecting VEGFR2 autophosphorylation, we carried out computer docking simulations for binding interactions of FC with the active sites of both kinases. The X-ray crystal structure of the active form of Src tyrosine kinase, 1Y57.pdb (26), was used and Surflex-Dock reasonably reproduced the binding mode and conformation of the crystal ligand with a root mean square deviation (RMSD) of 1.71 Å. For FAK, 2IJM.pdb<sup>5</sup> was used and the RMSD between the crystal ligand and



its docked conformation was 1.20 Å. Figure 5 (A and D) shows the active sites of Src and FAK, respectively, displaying the ATP-binding site and the presence of the hydrophobic pockets near the ATP-binding site in the crystal structure.

Docking simulation suggests that FC may bind to the ATP-binding site in two major binding poses for Src (Fig. 5B and C). The benzopyran-2-one moiety of FC occupies the deep hydrophobic pocket in both binding modes. FC seems to be able to form a hydrogen bond with Met341 (Fig. 5B), which is reported to be a key interacting residue with the adenine ring nitrogen of ATP (29). This hydrogen bond is maintained in one binding mode, but not in the other mode. Interestingly, a hydrogen bonding with Lys295, which has been reported to be an interaction partner of  $\alpha$ -phosphate group of ATP (27), is required in the latter binding mode (Fig. 5C).

For FAK, the benzopyran-2-one moiety of FC appears to occupy the region where the adenine part of ATP binds, maintaining the hydrogen bonding with Cys502. Figure 5 (E and F) shows the two possible binding poses of FC at the active site of FAK. However, FC may bind to active sites of FAK just like ATP without occupying the relatively shallow hydrophobic pocket of FAK, which differs from Src tyrosine kinase.

#### Comparison of FC Binding Sites in Src and FAK

To understand the structural basis for the potential binding differences of FC between Src and FAK, their crystal structures were aligned for comparison. Using the active Src kinase crystal structure (PDB ID: 1Y57) as a reference, the inactive Src kinase (PDB ID: 2H8H) and FAK (PDB ID: 2IJM) structures were aligned by sequence homology based on their  $\alpha$  carbons as shown in Supplementary Fig. S4A. In the active Src (displayed in cyan ribbon), SH2 and SH3 domains are displaced at right angles, allowing the kinase domain to open compared with the inactive Src kinase (displayed in blue ribbons), which is a compact form.

The sequence identity between the kinase domains of Src and FAK (displayed in green ribbon) is ~41%, and their overall secondary structures are also quite similar (to the RMSD of ~2.1 Å) based on their  $\alpha$  carbons. Src contains the characteristic deep hydrophobic pocket near the ATP-binding site. However, the shape and size of the hydrophobic pockets seem to be quite different between Src and FAK (Supplementary Fig. S4B–D). FC seems to easily bind into the hydrophobic pocket of Src, whereas the overall binding conformation of FC in FAK resembles that of ATP due to the spatial limitation of the pocket, suggesting the distinctively different binding modes of FC docking into Src and FAK. These predictions require experimental validation.

#### Discussion

Our results showed, to our knowledge for the first time, the antiangiogenic potential of FC isolated from

*F. assafoetida* L. in a number of cell culture assays using HUVECs as the endothelial cell targets. Importantly, the *in vitro* antiangiogenic actions of FC manifested with exposure concentrations at or below 40  $\mu$ mol/L, which did not cause cytotoxicity against non-angiogenically stimulated HUVECs. The battery of assays established the inhibition of the VEGF-induced tube formation on Matrigel (Fig. 1C) and the inhibitory effects of FC on the angiogenic responses of endothelial cells elicited by VEGF, including cell proliferation (Fig. 1D), migration (Fig. 2A), invasion through Matrigel (Fig. 2B), and expression of pro-MMP2 detectable by gelatin zymography (Fig. 2C). Each of these VEGF-stimulated processes (increment) was inhibited by FC with IC<sub>50</sub> of 10 to 20  $\mu$ mol/L in reference to the unstimulated baseline levels. We also confirmed the antiangiogenic potential observed in HUVEC models by the *ex vivo* rat aortic ring assay, which retained the three-dimensional tissue context and mixture of cell types (Fig. 2D).

We established, also for the first time, the *in vivo* anticancer efficacy of FC in the highly angiogenesis-dependent LLC allograft model, demonstrating a potent suppression of tumor growth implanted on the flank of syngenic mice (Fig. 3B), without adverse effect on the body weight of the hosts (Fig. 3A). It is noteworthy that the potency of the effective dose of 1 mg/kg body weight would be on par with or even better than the taxane drugs for *in vivo* anticancer activity in the same model (30). We chose the 1 mg/kg dose with the presumption of maximally achievable FC by i.p. delivery to be within the noncytotoxic range studied in the *in vitro* models to allow the antiangiogenesis actions to express. A direct measurement of the blood/serum or tumor tissue level of FC would be highly desirable to address the issue of its circulating and tissue-achievable levels for further mechanistic considerations. Nonetheless, the assumption seemed to bear out when we found by immunohistochemistry that the *in vivo* antitumor efficacy was associated with a reduction of intratumoral microvessel density (CD34 index for angiogenesis; Fig. 3C) and tumor cell proliferation (Ki-67 index; Fig. 3D), but without affecting TUNEL-positive apoptotic cells in the tumor sections (Fig. 3E).

Our study also provided novel and mechanistic insights into how FC targets multiple facets of vascular endothelial angiogenic signaling through the VEGFR1 and VEGFR2 axes. VEGFR2 has strong tyrosine kinase activity, transducing the major signals for vascular endothelial responses in angiogenesis (12, 15–17), including enhancing survival through activating PI3K-AKT, stimulating motility and actin reorganization through Rac as well as through p38 MAPK, and activation of ERK and DNA synthesis. There is now ample evidence that FAK and Src nonreceptor protein tyrosine kinases contribute to the endothelial responses (31–33). VEGFR2 transduces signals through FAK, and the phosphorylation of FAK on Tyr397 creates a high-affinity binding site recognized by the SH2 domain of Src family kinases and leads to the

activation of Src. Thus, activation of the FAK-Src complex is central to regulation of downstream signaling pathways that control angiogenesis events such as cell movement and survival. On the other hand, VEGFR1 plays a crucial role in negatively regulating angiogenesis in the embryo, most likely by trapping VEGF-A due to high affinity to prevent excessive signaling through VEGFR2 (17). VEGFR1 is now known to play a positive role in promoting tumor angiogenesis by cross-talks among epithelial cells and other cell types because VEGFR1 is expressed in not only endothelial cells but also macrophage-lineage cells and tumor epithelial cells and respond to other physiologic ligands placental growth factor and VEGF-B in autocrine and paracrine manners to promote tumor growth, metastasis, and inflammation (17).

On the one hand, FC interfered with binding of VEGF to VEGFR1/Flt-1 (Fig. 4A) and also reduced VEGFR1 autophosphorylation (Fig. 4B). These findings are consistent with the observation that FC directly targets the VEGFR1 axis at the receptor-ligand binding stage to decrease autophosphorylation. On the other hand, although FC did not affect VEGF binding to VEGFR2 (Fig. 4A) or its autophosphorylation (Fig. 4B), the observed reduction of VEGF-induced phosphorylation of FAK-Src signaling pathways in VEGF-treated HUVECs and the observed suppression of ERK, p38 MAPK, and JNK phosphorylation without affecting pAKT implicate the possible selective and multiple targeting of the VEGFR2 downstream pathways, but not VEGFR2 ligand binding per se. Consistent with this notion, molecular modeling studies suggest that FC could inhibit Src kinase and FAK activity through its direct docking into the ATP-binding sites of these target proteins (Fig. 5), although the binding modes of FC to the active sites of Src and FAK were projected to be quite different (Supplementary Fig. S4). Proof of direct inhibitory action of FC on Src and FAK and the inhibition kinetics are to be obtained to substantiate the predictions.

Further computational analyses comparing the VEGFR1 and VEGFR2 structures might yield useful insights into the molecular basis of the differential targeting by FC of these two receptors. However, the lack of published protein crystal data for VEGFR1 has limited our attempt with this approach. It is known that VEGFR1

binds VEGF with at least 10 times higher affinity than does VEGFR2 (12, 17). Future work should examine whether the specific inhibitory action of FC on VEGF-A/VEGFR1 binding and signaling is applicable to other cell types that express this receptor to evaluate the merit of FC to affect cross-talks among endothelial and many other cell types that contribute to tumor angiogenesis and escapes from VEGF-A/VEGFR2-targeted anti-angiotherapies (17). Inactivating antibodies against VEGFR1 (16) or its other ligand PlGF (17) have shown significant antitumor activities in preclinical models, supporting the crucial role of targeting this signaling axis in other cell types as well as in vascular endothelial cells toward improving the overall efficacy of treating cancer-associated angiogenesis.

In conclusion, FC targets a number of angiogenesis signaling molecules/pathways involving endothelial cell proliferation, migration, invasion, and the expression of MMP-2 and tube formation of VEGF-induced HUVECs *in vitro* and inhibits the *ex vivo* angiogenic sprouting in the aortic ring assay. Mechanistic investigations reveal that FC may target multiple aspects of kinase signaling cascades of the VEGFR1 and VEGFR2 (FAK/Src) axes, likely through distinct mechanisms that remain to be further defined. These findings suggest that the strong anti-angiogenic activity of FC may principally mediate its anticancer activity *in vivo*. FC merits further investigation as a novel candidate agent for antiangiogenic therapy, especially for complementing current VEGF-A/VEGFR2 targeting modalities.

#### Disclosure of Potential Conflicts of Interest

No potential conflicts of interest were disclosed.

#### Grant Support

Medical Research Center grant 2009-0063466 (S.H. Kim) and Hormel Foundation (J. Lu).

The costs of publication of this article were defrayed in part by the payment of page charges. This article must therefore be hereby marked *advertisement* in accordance with 18 U.S.C. Section 1734 solely to indicate this fact.

Received 8/21/09; revised 11/11/09; accepted 11/24/09; published OnlineFirst 1/26/10.

#### References

- Unnikrishnan MCKR. Tumour reducing and anticarcinogenic activity of selected spices. *Cancer Lett* 1990;51:85–9.
- Soni KB, Lahiri M, Chackradeo P, Bhide SV, Kuttan R. Protective effect of food additives on aflatoxin-induced mutagenicity and hepatocarcinogenicity. *Cancer Lett* 1997;115:129–33.
- Rollinger JM, Steindl TM, Schuster D, et al. Structure-based virtual screening for the discovery of natural inhibitors for human rhinovirus coat protein. *J Med Chem* 2008;51:842–51.
- Nam NH, Kim Y, You YJ, Hong DH, Kim HM, Ahn BZ. New constituents from *Crinum latifolium* with inhibitory effects against tube-like formation of human umbilical venous endothelial cells. *Nat Prod Res* 2004;18:485–91.
- Lee S, Sivakumar K, Shin WS, Xie F, Wang Q. Synthesis and anti-angiogenesis activity of coumarin derivatives. *Bioorg Med Chem Lett* 2006;16:596–9.
- Bobek V, Kovarik J. Antitumor and antimetastatic effect of warfarin and heparins. *Biomed Pharmacother* 2004;58:13–19.
- Nakashima T, Hirano S, Agata N, et al. Inhibition of angiogenesis by a new isocoumarin, NM-3. *J Antibiot (Tokyo)* 1999;52:426–8.
- Folkman J, Shing Y. Angiogenesis. *J Biol Chem* 1992;267:10931–4.
- Folkman J. Tumor angiogenesis: therapeutic implications. *N Engl J Med* 1971;285:1182–6.
- Carmeliet P. Mechanisms of angiogenesis and arteriogenesis. *Nat Med* 2000;6:389–95.

11. Fischer C, Schneider M, Carmeliet P. Principles and therapeutic implications of angiogenesis, vasculogenesis and arteriogenesis. *Handb Exp Pharmacol* 2006;176:157–212.
12. Kowanetz M, Ferrara N. Vascular endothelial growth factor signaling pathways: therapeutic perspective. *Clin Cancer Res* 2006;12:5018–22.
13. Keck PJ, Hauser SD, Krivi G, et al. Vascular permeability factor, an endothelial cell mitogen related to PDGF. *Science* 1989;246:1309–12.
14. Houck KA, Ferrara N, Winer J, Cachianes G, Li B, Leung DW. The vascular endothelial growth factor family: identification of a fourth molecular species and characterization of alternative splicing of RNA. *Mol Endocrinol* 1991;5:1806–14.
15. Bernatchez PN, Soker S, Sirois MG. Vascular endothelial growth factor effect on endothelial cell proliferation, migration, and platelet-activating factor synthesis is Flk-1-dependent. *J Biol Chem* 1999;274:31047–54.
16. Ellis LM, Hicklin DJ. VEGF-targeted therapy: mechanisms of anti-tumour activity. *Nat Rev Cancer* 2008;8:579–91.
17. Fischer C, Mazzone M, Jonckx B, Carmeliet P. FLT1 and its ligands VEGFB and PlGF: drug targets for anti-angiogenic therapy? *Nat Rev Cancer* 2008;8:942–56.
18. Huh JE, Lee EO, Kim MS, et al. Penta-O-galloyl- $\beta$ -D-glucose suppresses tumor growth via inhibition of angiogenesis and stimulation of apoptosis: roles of cyclooxygenase-2 and mitogen-activated protein kinase pathways. *Carcinogenesis* 2005;26:1436–45.
19. Lee SJ, Lee HM, Ji ST, Lee SR, Mar W, Gho YS. 1,2,3,4,6-Penta-O-galloyl- $\beta$ -D-glucose blocks endothelial cell growth and tube formation through inhibition of VEGF binding to VEGF receptor. *Cancer Lett* 2004;208:89–94.
20. Lee HJ, Lee EO, Rhee YH, et al. An oriental herbal cocktail, ka-mi-kae-kyuk-tang, exerts anti-cancer activities by targeting angiogenesis, apoptosis and metastasis. *Carcinogenesis* 2006;27:2455–63.
21. Son SH, Kim MJ, Chung WY, et al. Decursin and decursinol inhibit VEGF-induced angiogenesis by blocking the activation of extracellular signal-regulated kinase and c-Jun N-terminal kinase. *Cancer Lett* 2009;280:86–92.
22. Jung MH, Lee SH, Ahn EM, Lee YM. Decursin and decursinol angelate inhibit VEGF-induced angiogenesis via suppression of the VEGFR-2-signaling pathway. *Carcinogenesis* 2009;30:655–61.
23. Liang CC, Park AY, Guan JL. In vitro scratch assay: a convenient and inexpensive method for analysis of cell migration *in vitro*. *Nat Protoc* 2007;2:329–33.
24. Jiang C, Ganther H, Lu J. Monomethyl selenium-specific inhibition of MMP-2 and VEGF expression: implications for angiogenic switch regulation. *Mol Carcinog* 2000;29:236–50.
25. Kruger EA, Duray PH, Tsokos MG, et al. Endostatin inhibits microvessel formation in the *ex vivo* rat aortic ring angiogenesis assay. *Biochem Biophys Res Commun* 2000;268:183–91.
26. Cowan-Jacob SW, Fendrich G, Manley PW, et al. The crystal structure of a c-Src complex in an active conformation suggests possible steps in c-Src activation. *Structure* 2005;13:861–71.
27. Xu W, Doshi A, Lei M, Eck MJ, Harrison SC. Crystal structures of c-Src reveal features of its autoinhibitory mechanism. *Mol Cell* 1999;3:629–38.
28. Jain AN. Surflex: fully automatic flexible molecular docking using a molecular similarity-based search engine. *J Med Chem* 2003;46:499–511.
29. Hennequin LF, Allen J, Breed J, et al. *N*-(5-chloro-1,3-benzodioxol-4-yl)-7-[2-(4-methylpiperazin-1-yl)ethoxy]-5-(tetrahydro-2*H*-pyran-4-yloxy)quinazolin-4-amine, a novel, highly selective, orally available, dual-specific c-Src/Abl kinase inhibitor. *J Med Chem* 2006;49:6465–88.
30. Bissery MC, Guenard D, Gueritte-Voegelein F, Lavelle F. Experimental antitumor activity of taxotere (RP 56976, NSC 628503), a Taxol analogue. *Cancer Res* 1991;51:4845–52.
31. Abedi H, Zachary I. Vascular endothelial growth factor stimulates tyrosine phosphorylation and recruitment to new focal adhesions of focal adhesion kinase and paxillin in endothelial cells. *J Biol Chem* 1997;272:15442–51.
32. Abu-Ghazaleh R, Kabir J, Jia H, Lobo M, Zachary I. Src mediates stimulation by vascular endothelial growth factor of the phosphorylation of focal adhesion kinase at tyrosine 861, and migration and anti-apoptosis in endothelial cells. *Biochem J* 2001;360:255–64.
33. Parsons JT, Martin KH, Slack JK, Taylor JM, Weed SA. Focal adhesion kinase: a regulator of focal adhesion dynamics and cell movement. *Oncogene* 2000;19:5606–13.

# Molecular Cancer Therapeutics

## Herbal Compound Farnesiferol C Exerts Antiangiogenic and Antitumor Activity and Targets Multiple Aspects of VEGFR1 (Flt1) or VEGFR2 (Flk1) Signaling Cascades

Jae-Ho Lee, Sun Choi, Yoonji Lee, et al.

*Mol Cancer Ther* 2010;9:389-399. Published OnlineFirst January 26, 2010.

<b>Updated version</b>	Access the most recent version of this article at: <a href="https://doi.org/10.1158/1535-7163.MCT-09-0775">doi:10.1158/1535-7163.MCT-09-0775</a>
<b>Supplementary Material</b>	Access the most recent supplemental material at: <a href="http://mct.aacrjournals.org/content/suppl/2010/01/25/1535-7163.MCT-09-0775.DC1">http://mct.aacrjournals.org/content/suppl/2010/01/25/1535-7163.MCT-09-0775.DC1</a>

<b>Cited articles</b>	This article cites 33 articles, 6 of which you can access for free at: <a href="http://mct.aacrjournals.org/content/9/2/389.full#ref-list-1">http://mct.aacrjournals.org/content/9/2/389.full#ref-list-1</a>
-----------------------	---

<b>E-mail alerts</b>	<a href="#">Sign up to receive free email-alerts</a> related to this article or journal.
<b>Reprints and Subscriptions</b>	To order reprints of this article or to subscribe to the journal, contact the AACR Publications Department at <a href="mailto:pubs@aacr.org">pubs@aacr.org</a> .
<b>Permissions</b>	To request permission to re-use all or part of this article, use this link <a href="http://mct.aacrjournals.org/content/9/2/389">http://mct.aacrjournals.org/content/9/2/389</a> . Click on "Request Permissions" which will take you to the Copyright Clearance Center's (CCC) Rightslink site.